ADVANCED HEALTHCARE MATERIALS
www.advhealthmat.de

Directing Valvular Interstitial Cell Myofibroblast-Like Differentiation in a Hybrid Hydrogel Platform

Jesper Hjortnaes, Gulden Camci-Unal, Joshua D. Hutcheson, Sung Mi Jung, Frederick J. Schoen, Jolanda Kluin, Elena Aikawa, and Ali Khademhosseini**

Three dimensional (3D) hydrogel platforms are powerful tools, providing controllable, physiologically relevant microenvironments that could aid in understanding how various environmental factors direct valvular interstitial cell (VIC) phenotype. Continuous activation of VICs and their transformation from quiescent fibroblast to activated myofibroblast phenotype is considered to be an initiating event in the onset of valve disease. However, the relative contribution VIC phenotypes is poorly understood since most 2D culture systems lead to spontaneous VIC myofibroblastic activation. Here, a hydrogel platform composed of photocrosslinkable versions of native valvular extracellular matrix components—methacrylated hyaluronic acid (HAMA) and methacrylated gelatin (GelMA)—is proposed as a 3D culture system to study VIC phenotypic changes. These results show that VIC myofibroblast-like differentiation occurs spontaneously in mechanically soft GelMA hydrogels. Conversely, differentiation of VICs encapsulated in HAMA-GelMA hybrid hydrogels, does not occur spontaneously and requires exogenous delivery of TGFβ1, indicating that hybrid hydrogels can be used to study cytokine-dependent transition of VICs. This study demonstrates that a hybrid hydrogel platform can be used to maintain a quiescent VIC phenotype and study the effect of environmental cues on VIC activation, which will aid in understanding pathobiology of valvular disease.

1. Introduction

Heart valves contain valvular interstitial cells (VICs), a heterogeneous cell population that maintains tissue homeostasis and structural integrity of the heart valve leaflet extracellular matrix (ECM).[1] In native healthy heart valves, VICs are mostly described as having a quiescent fibroblast-like phenotype; however, upon stimulation by environmental cues, VICs can differentiate into myofibroblast-like cells. Activated VICs, hallmarked by alpha smooth muscle actin (α-SMA) expression, play an important role in valve tissue remodeling that is characterized by increased deposition of ECM proteins such as collagen, elastin, and glycosaminoglycans (GAGs), and overexpression of matrix metalloproteinases (MMPs), cathepsins, and tissue inhibitors.[1a,2] Persistent activation of VICs results in pathological remodeling of the valve matrix, in part attributed to valvular fibrosis.[1b] Moreover, activated VICs

J. Hjortnaes, Dr. G. Camci-Unal, Prof. A. Khademhosseini
Biomaterials Innovation Research Center
Division of Biomedical Engineering
Department of Medicine
Brigham and Women's Hospital
Harvard Medical School
Boston, MA, USA
E-mail: alik@rics.bwh.harvard.edu

J. Hjortnaes, Prof. E. Aikawa
Center of Excellence in Vascular Biology
Department of Cardiovascular Medicine
Brigham and Women's Hospital
Harvard Medical School
Boston, MA, USA
E-mail: eaikawa@partners.org

J. Hjortnaes, Dr. J. Kluin
Department of Cardiothoracic Surgery
University Medical Center Utrecht
Utrecht, The Netherlands

Dr. G. Camci-Unal, Prof. A. Khademhosseini
Harvard-MIT Division of Health Sciences and Technology
Massachusetts Institute of Technology
Cambridge, MA, USA

Dr. J. D. Hutcheson, Prof. E. Aikawa
Center for Interdisciplinary Cardiovascular Sciences
Brigham and Women's Hospital
Harvard Medical School
Boston, MA, USA

DOI: 10.1002/adhm.201400029

Dr. S. M. Jung
Department of Electrical Engineering
and Computer Science
Massachusetts Institute of Technology
Cambridge, MA, USA

Prof. F. J. Schoen
Department of Pathology
Brigham and Women's Hospital
Harvard Medical School
Boston, MA, USA

Prof. A. Khademhosseini
Wyss Institute for Biologically Inspired Engineering
Harvard University
Boston, MA, USA

Prof. A. Khademhosseini
Department of Maxillofacial Biomedical Engineering and
Institute of Oral Biology
School of Dentistry
Kyung Hee University
Seoul, Republic of Korea

Prof. A. Khademhosseini
Department of Physics
King Abdulaziz University
Jeddah, Saudi Arabia

are believed to play an active role in calcific aortic valve disease, in which myofibroblast-like cells differentiate into osteoblast-like cells resulting in calcium deposition.[3] However, regulation of the phenotypic changes in VICs and the role of VICs in tissue homeostasis during healthy and pathological remodeling are poorly understood. One major problem that has hindered research into valvular homeostasis and remodeling is the lack of a suitable in vitro system to study VIC behavior. Culturing VICs on tissue culture polystyrene has been shown to promote myofibroblastic activation.

In addition, although animal models such as murine,[2a] rabbit,[4] and porcine[5] exist that simulate aortic valve disease, they often fail to develop significant stenosis, which is characteristic of human aortic valve disease. Furthermore, these models are mostly based on hypercholesterolemia and subsequent atherosclerosis, which currently is viewed as a different etiology to calcific aortic valve disease.[3c]

In order to better understand pathologic changes in VIC phenotype, several studies have utilized bio-mimetic in vitro model systems that support physiological quiescence of VICs and do not directly promote VIC differentiation to activated myofibroblast-like cells.[6] An appropriate model system would closely simulate tissue homeostasis in order to monitor changes in VIC phenotype as homeostasis is perturbed. Understanding the mechanisms involved in VIC regulation of tissue homeostasis may not only elucidate the mechanisms of valve disease but also aid in the engineering of tissue valve substitutes and development of drug screening tools.

Cell–ECM interactions are important components of VIC regulation, with biomechanical signaling from deformation or changes in mechanical stiffness of the ECM playing a key role in modulating VIC phenotype.[7] External mechanical forces such as shear stress, pressure, and stretch are transmitted through the ECM to the VICs and likely elicit cellular responses that drive homeostasis and disease.[8] Similarly, the intrinsic stiffness of the ECM can regulate cell function and modulate the response of VICs to other environmental stimuli. Cells can sense the local stiffness of the ECM by pulling on the substrate at focal adhesions.[9] Cells respond to stiffness of a substrate by altering integrin expression, focal adhesions, and cytoskeletal organization to establish a force balance between the resistance provided by the substrate and the cell-generated traction force.[10] In turn, these processes regulate intracellular signaling pathways, making cells sensitive to the surrounding stiffness.[11] To this point, 2D in vitro studies with VICs cultured on tunable substrates have predominantly shown myofibroblast-like differentiation on stiffer substrates.[6a,7] However, VIC activation has recently also been shown to occur in on soft substrates, with a phenotypic change threshold value at ≈15 kPa.[6a] Therefore, further characterization of VIC responses to substrate mechanics is needed to understand the process of myofibroblast differentiation. Most knowledge on this interaction is based on 2D-culture studies, which are not appropriate representations of the in vivo microenvironment.

Hydrogel-based 3D culture platforms can provide for a more tissue-like environment to study VIC behavior due to their potential to mimic the natural ECM of specific tissues. Previously, VICs have been cultured within 3D matrices derived from natural ECM polymers such as commonly used collagen and fibrin.[12] Although these matrices are able to facilitate good viability, collagen and fibrin gels seeded with VICs are increasingly susceptible to degradation and compaction, due to the contractile nature and expression of remodeling enzymes by activated VICs.[13] In addition, natural-protein-based gels may initiate various cell-signaling cascades and are associated with sequestering growth factors and cytokines from media, providing for added complexity in isolating specific material-guided effects on VIC function over time. To this end, photocrosslinking has been used to engineer controllable and tunable hydrogels from naturally derived ECM polymers.[14] Using modified naturally derived polymers such as gelatin or hyaluronic acid, cells can be encapsulated under relatively mild conditions, limiting cell damage.[15] Methacrylated gelatin (GelMA)[14b] has successfully been used as a platform to investigate VIC fate,[15b] which suggests the potential of this material for development of heart valve-like culture models. However, GelMA alone is a relatively weak material that quickly degrades even without cells, and thus poses challenges to longer experimental times. Furthermore, GelMA is susceptible to contraction by myofibroblast-like cells, which warrants the addition of another polymer component to strengthen this hydrogel network. Methacrylated hyaluronic acid (HAMA) has similarly been explored as a photocrosslinkable material for VIC-laden hydrogels.[15c,16] Hyaluronic acid is an important ECM of the adult heart valve and is a vital component of the cardiac jelly during heart embryogenesis. Therefore, hyaluronic acid is a critical ECM component needed to create a physiological representative environment to study VIC behavior. However, HAMA-based hydrogels have demonstrated limited cell adhesiveness, which results in restricted cell spreading.[15c,17] Conversely, it has been shown that by adding HAMA to collagen, the formation of a collagen fiber network is altered to such an extent that the compaction of gels is impaired, compared to collagen gels alone.[18] In addition, due to the slow degradation of HAMA,[19] it may increase the structural integrity of the hydrogel for long experiments.

In this paper, we aimed to combine the unique advantages of GelMA and HAMA, two naturally derived materials, into a hybrid hydrogel platform, which is more analogous to the native valve ECM environment. By changing the concentration of polymers in the hydrogels, we aimed to develop a platform that could be used to maintain quiescence of VICs and study the effect of various environmental cues on VIC differentiation into myofibroblast-like cells. Such a platform may be a useful tool to understand valvular pathobiology, and importantly aid in the development of drug discovery platforms.

2. Results

2.1. Material Characteristics of Hydrogel Compositions

Scanning electron microscopy images of cross-sections of the various single-component hydrogel conditions demonstrate different porosities characteristic of each hydrogel condition (**Figure 1**D). These images reveal that pore sizes decrease with increased hydrogel macromer concentrations. Significant differences are observed in the swelling ratio of each

DOI: 10.1002/adhm.201400029

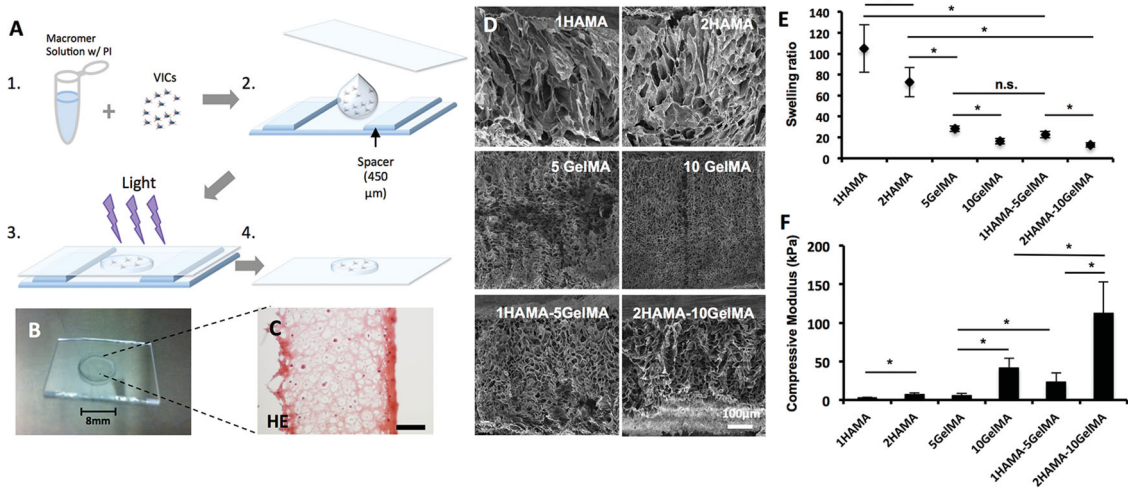

Figure 1. Fabrication and characterization of VIC-laden hydrogels**.** A) VICs are isolated and resuspended in macromer solution, which consists of HAMA and/or GelMA in 0.5% photoinitiator (Igracure 2595) solution. Fifty microliters prepolymer solution is put onto a sterile mold between two spacers of 450 μm and covered with sterile glass slide, which is subsequently crosslinked by exposure to light (365 nm) for 30 s at intensity of 2.5 mW cm^{-2}. Cell-laden hydrogels are removed from the glass slide and cultured according to protocol. B) Hematoxylin and eosin stain of VIC-laden hydrogel. C) Macroscopic image of VIC-laden hydrogel on glass slide. D) Scanning electron microscopy (Ultra 55, Carl Zeiss, NY, USA, 5.0 kV) images of different hydrogel compositions. Bar: 100 μm. E) Swelling ratio of hybrid hydrogels (Swelling ratio = Wet weight–dry weight/dry weight). F) Compressive modulus was calculated using compressive uniaxial test. 2% (w/v) HAMA-10% (w/v) GelMA demonstrated the highest modulus. Data are depicted as mean ± SD, *$p < 0.05$.

hydrogel condition, indicating that porosity is tunable by varying the concentration of polymer in the hydrogel (Figure 1E). Increasing the concentration of 1% (w/v) HAMA to 2% (w/v) HAMA resulted in a significant decrease in the swelling ratio of approximately 30%, ($p < 0.05$). A similar decrease of 30% ($p < 0.05$) occurred with an increased macromer concentration from 5% (w/v) GelMA to 10% (w/v) GelMA. In addition, GelMA hydrogels proved to be less porous than HAMA hydrogels ($p < 0.05$).

The swelling ratios of the hybrid hydrogels 1% (w/v) HAMA-5% (w/v) GelMA and 2% (w/v) HAMA-10% (w/v) GelMA were 22 ± 3 and 12 ± 2, respectively. As such, when combining these HAMA and GelMA polymers together their swelling ratios are close to their separate GelMA counterparts 5% (w/v) (23 ± 10) and 10% (w/v) GelMA (16 ± 2). Notably, there is a significant difference in swelling ratio between 10% (w/v) GelMA and 2% (w/v) HAMA-10% (w/v) GelMA; however, there is no significant difference ($p = 0.45$) in swelling ratio between the 1% (w/v) HAMA-5% (w/v) GelMA hybrid and 5% (w/v) GelMA only. Pore sizes were also quantified using SEM images to determine ECD (Figure I, Supporting Information), which also revealed no significant difference between 5% (w/v) GelMA hydrogels and 1% (w/v) HAMA-5% (w/v) GelMA hydrogels.

An increase in HAMA or GelMA concentration facilitated an increase in compressive moduli. Similarly, we observed elevated hydrogel stiffness—described as compressive modulus—with increased total concentration of polymers in hybrid hydrogels (Figure 1F). As such, 2% (w/v) HAMA-10% (w/v) GelMA demonstrated the highest compressive modulus compared to all other conditions ($p < 0.05$). All conditions were significantly different ($p < 0.05$). These results verify the inverse relationship of porosity and stiffness of the independent HAMA- and GelMA-based hydrogels with increasing the polymer concentrations. However, although we observed a significant increase in stiffness when HAMA is added to GelMA, a relative small and non-significant change in porosity occurs.

2.2. VIC Viability, Spreading, and Proliferation in Hydrogel Composites

After 21 d of culture, VICs encapsulated in the various hydrogel conditions were evaluated for cell viability and compared to day 1. **Figure 2**A depicts representative cross-sections of the middle portion of the hydrogel from z-stacks obtained by confocal microscopy after live/dead staining. Overall, cell viability remained high (>80%). However, VICs encapsulated in 2% (w/v) HAMA-10% (w/v) GelMA hydrogels were less viable compared to 1% (w/v) HAMA-5% (w/v) GelMA hydrogels (77.7 ± 6.1 vs 87.4 ± 2.4, $p < 0.05$) (Figure 2B). In addition, TUNEL staining performed on sections of VIC-laden hydrogels at day 21 demonstrated no apoptotic cells compared to positive control (Supplemental Figure II, Supporting Information). Notably, as visualized by live/dead staining, VICs seemed to spread more when encapsulated in 5% (w/v) GelMA hydrogels (Figure 2A). This is confirmed by quantifying surface area as depicted in Figure 2C, demonstrating a significantly higher mean surface area in 5% (w/v) GelMA hydrogels (169.1 ± 69.3 μm^2) compared to the other conditions (1% (w/v) HAMA; 13.8 ± 2.2 μm^2, 2%(w/v) HAMA: 26.1 ± 1.9 μm^2, 10% (w/v) GelMA: 21.4 ± 10.4 μm^2, 1% (w/v) HAMA-5% (w/v) GelMA: 29.1 ± 8.7 μm^2, and 2% (w/v) HAMA-10% (w/v) GelMA: 18.3 ± 5.0 μm^2, respectively).

Proliferation was assessed by EdU labeling. **Figure 3**A demonstrates representative cross-sections of the middle of the hydrogel as imaged by confocal microscopy. The bottom panels

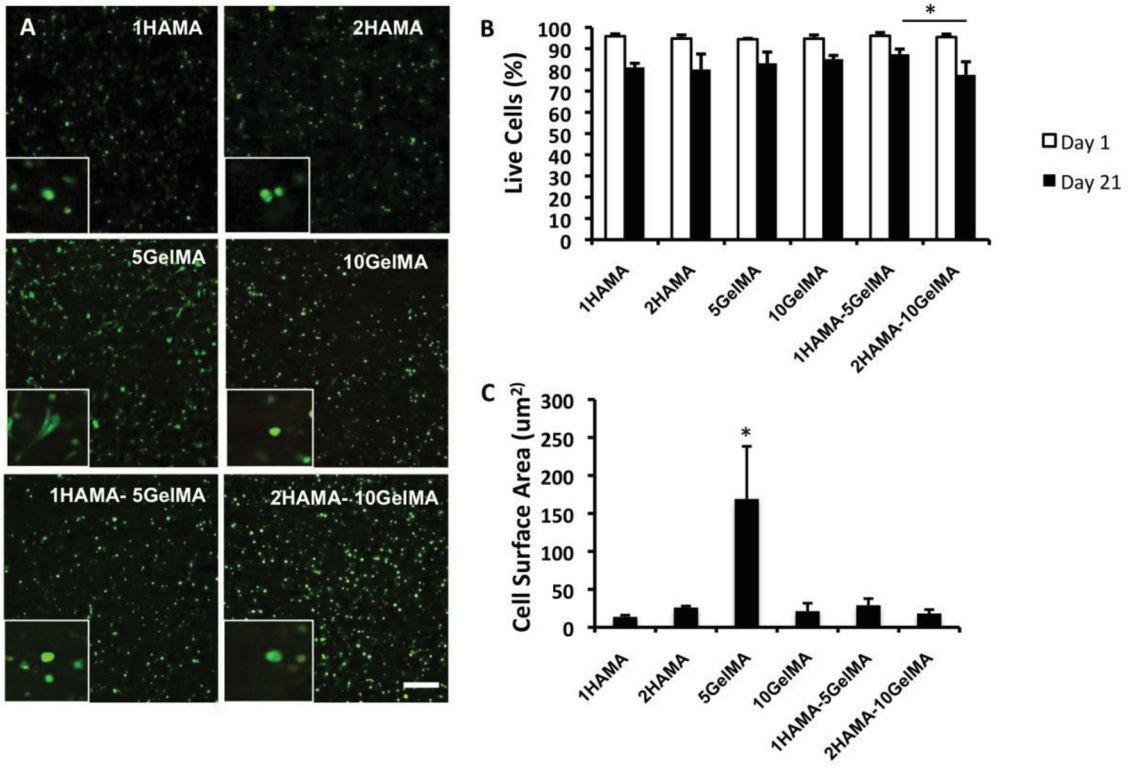

Figure 2. Hydrogel conditions maintain high viability and affects spreading**.** VIC-laden hydrogels were cultured up to 21 d. A) Representative confocal images of live/dead stain of hydrogel conditions at day 21; bar: 50 μm. B) Quantification of % live cells as determined from confocal z-stacks made from hydrogels ($n = 3$). C) Quantification of cell spreading per hydrogel condition (mean cell surface area). Data are depicted as mean ± SD. *$p < 0.05$.

demonstrate control images of the cells populating the surface of 5% (w/v) GelMA and a positive control, which was obtained after 24 h of culture in normal growth media after seeding. Using z-stack analysis of EdU-labeled cells in hydrogels allows for evaluating proliferation of encapsulated cells.

The percentage of EdU expressing cells in 1% (w/v) HAMA was 61 ± 13% after 1 d and 47 ± 8% after 21 d of culture, but was not statistically significant. In 2% (w/v) HAMA hydrogels, VICs expressing EdU remained similar after 21 d of culture (day 1: 42 ± 7%, day 21: 46 ± 9%). However in 5% (w/v) GelMA, there was a significant decrease in EdU expression at day 7 (32 ± 4%), day 14 (35 ± 7%), day 21 (30 ± 9%) compared to day 1 (47 ± 8%), $p < 0.05$). In addition, the amount of VICs encapsulated in 5% (w/v) GelMA labeled with EdU was significantly lower at days 14 and 21 compared to VICs encapsulated in all other hydrogel conditions ($p < 0.05$). EdU expression in 10% (w/v) GelMA remained statistically similar after 21 d of culture. 1% (w/v) HAMA-5% (w/v) GelMA cell-laden hydrogels demonstrated EdU expressing VICs of day 1: 45 ± 5%, day 7: 37 ± 5%, day 14: 61 ± 7% and day 21: 60 ± 11%, where days 14 and 21 were significantly increased compared to days 1 and 7 ($p < 0.05$).

Furthermore, we observed a significant decrease of the number of cells stained for DAPI in 1% (w/v) HAMA hydrogels after 21 days (120 ± 10) of culture compared to day 1 (286 ± 49), ($p < 0.05$) (Figure III, Supporting Information). A similar trend is observed in 2% (w/v) HAMA hydrogels with a decrease of cell number after 21 days of culture (302 ± 31 vs 158 ± 8, $p < 0.05$). In 5% (w/v) GelMA hydrogels, we observed an initial drop of cell number after day 1, but at day 21 the amount of cells was relatively similar (315 ± 55 vs 351 ± 38, $p > 0.05$). 10% (w/v) GelMA hydrogels demonstrated a decrease in cell number after 21 days, 366 ± 31 to 265 ± 28, $p < 0.05$. Cell number remained similar in 2% (w/v) HAMA-10% (w/v) GelMA: day 21: 332 ± 31 versus day 1:372 ± 36, $p > 0.05$.

2.3. VIC Behavior in Response to Hydrogel Composition

After 21 d of culture, encapsulated VICs were analyzed for their phenotypic responses to the hydrogel conditions. VICs demonstrated a myofibroblast-like phenotype characterized by positive immunofluorescence staining of α-SMA in 5% (w/v) GelMA hydrogels (**Figure 4**A). VICs in these gels exhibited a spread-like morphology (Figure 4A inserts) compared to VICs cultured in all other hydrogels. This phenotypic differentiation was confirmed by RT-PCR (Figure 4C) showing a significant increase in α-SMA mRNA expression of VICs in 5% (w/v) GelMA hydrogels (8.2 ± 2.9, $p < 0.05$) relative to VICs encapsulated in 1% (w/v) HAMA. Vimentin, a general mesenchymal cell marker, was positively expressed by VICs in all hydrogel conditions (Figure 4B) and similarly confirmed by no significant change in mRNA expression across all groups (Figure 4D), indicating that VICs remain quiescent

DOI: 10.1002/adhm.201400029

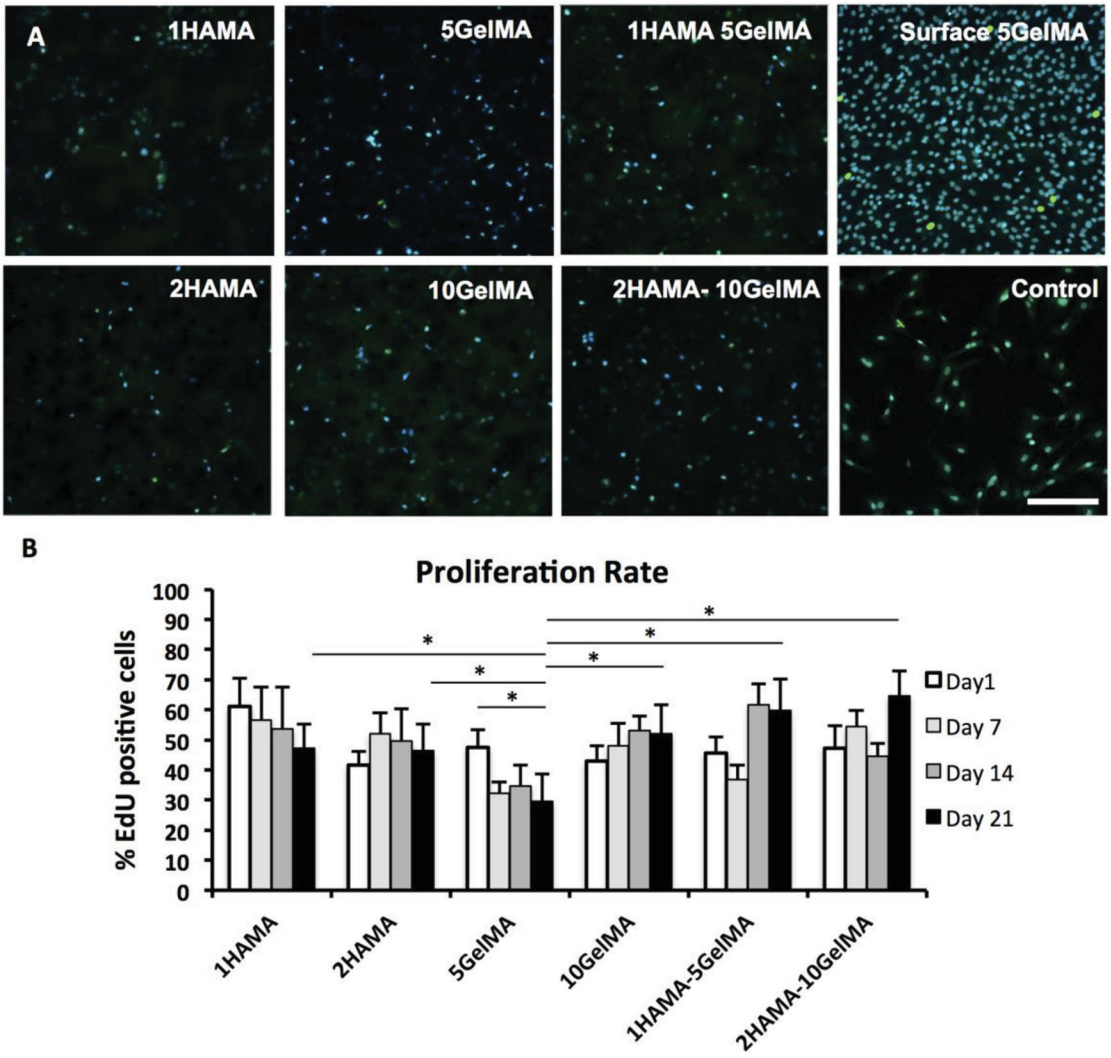

Figure 3. Proliferation of encapsulated VICs**.** VIC-laden hydrogels were cultured up to 21 d and analyzed for proliferation. A) Representative confocal images of EdU click-it labeling of encapsulated VICs. Image of cells on surface of 5% (w/v) GelMA. Positive control was obtained by culturing VICs for 24 h in medium containing 10% FBS. bar: 50 μm. B) Quantification of encapsulated proliferating cells as determined by positive EdU labeling in different hydrogel conditions at days 1, 7, 14, and 21, ($n = 3$). Data are depicted as mean ± SD. *$p < 0.05$.

fibroblast-like cells in most hydrogel conditions when cultured in normal media. In contrast, VICs cultured on TCPS (2D) mostly exhibited myofibroblast-like differentiation indicated by positive α-SMA and vimentin stain (Figure IV, Supporting Information).

However 5% (w/v) GelMA hydrogels seem to facilitate myofibroblast-like differentiation of VICs. In addition to elevated α-SMA, VICs in 5% GelMA exhibit an increased expression of MMP-9 as demonstrated by immunofluorescence (**Figure 5**A) and mRNA expression (fold change compared to 1% (w/v) HAMA: 4.4 ± 0.7, $p < 0.05$) (Figure 5C). Similarly VICs encapsulated in 5% (w/v) GelMA hydrogels exhibit increased expression of collagen type 1 (Figure 5B). RT-PCR quantification of collagen type 1 mRNA expression revealed (Figure 5D) a similar fold change compared to 1% (w/v) HAMA of all conditions containing GelMA ($p > 0.05$).

2.4. Quiescent VIC to Activated VIC Myofibroblast-Like Differentiation

After observing the quiescent nature of VICs in the hybrid hydrogels, we added TGFβ at 5 ng mL^{-1} to the culture medium for 21 d to 1% (w/v) HAMA-5% (w/v) GelMA hydrogels. We detected activated VICs encapsulated in 1% (w/v) HAMA-5% (w/v) GelMA hydrogels as depicted by positive immunofluorescence staining of α-SMA, vimentin, MMP-9, and Col1A1 similar to results for 5% (w/v) GelMA alone (**Figure 6**A). In addition, mRNA expression levels of α-SMA (41.8 ± 4.1), vimentin (4.5 ± 0.3), MMP-9 (6.7 ± 1.1), and COL1A1 (14.9 ± 2.3) were increased compared to control medium, indicating a myofibroblast-like differentiation of encapsulated VICs in the 1% (w/v) HAMA-5% (w/v) GelMA hydrogels when stimulated with TGFβ1 (Figure 6B).

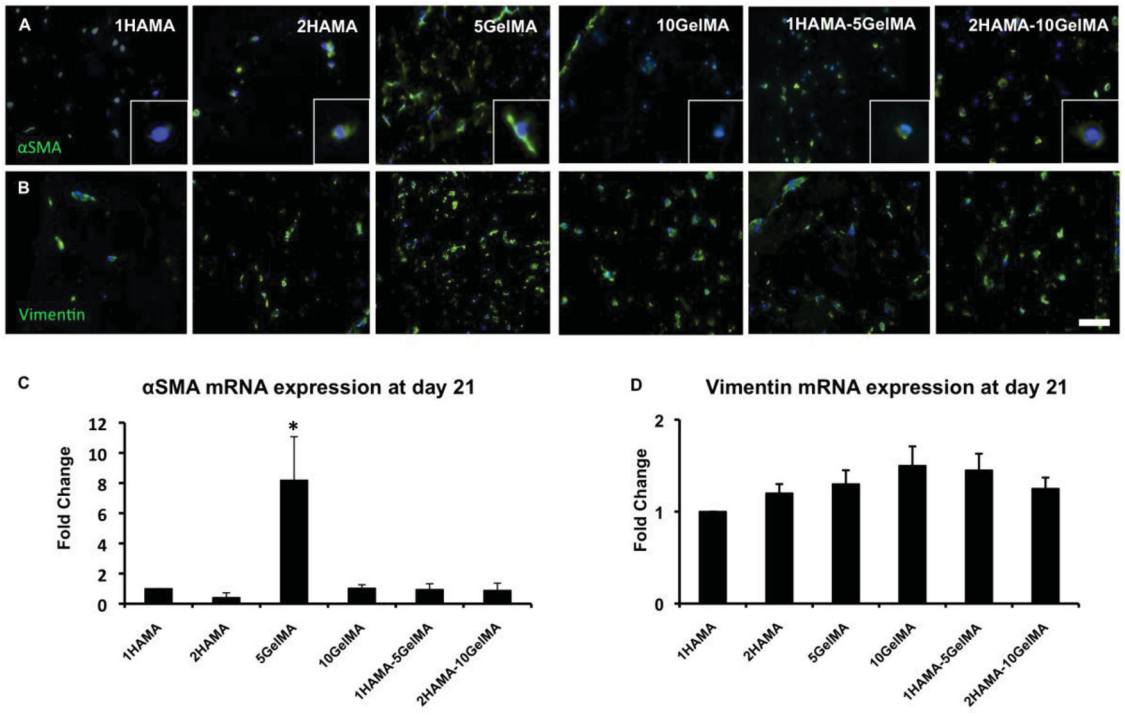

Figure 4. Hydrogel composition affects myofibroblast-like phenotype of VICs at day 21. A) Immunofluorescence staining of alpha smooth muscle actin (α-SMA) in all VIC-laden hydrogel conditions. α-SMA: green, nuclei: blue, Inserts: 40×, B) Immunofluorescence staining of vimentin; Vimentin: green, nuclei: blue, bar: 50 μm. C) mRNA expression assessed by RT-PCR of αSMA and D) vimentin. Expression is depicted as mean ± SD fold change to 1% (w/v) HAMA. $^*p < 0.05$.

3. Discussion

Engineered 3D culture platforms, such as hydrogels, have emerged as powerful tools to understand valvular biology, as they potentially provide physiologically relevant environments.[14a] Hydrogel systems allow for the creation of tunable 3D environments, by changing their parameters to regulate cellular responses. This has become particularly important for studying valve biology in vitro, since VICs cultured on stiff tissue culture plates spontaneously develop an activated myofibroblast-like phenotype, characteristic of a "disease"-like state.

By using naturally derived polymers, which are present in the native heart valve ECM, we aimed to develop a more physiologically relevant culture platform for VICs. In this study, we developed a tunable 3D hydrogel platform to analyze the phenotypic changes of VICs in response to hydrogel composition. We have demonstrated that by changing the relative concentrations of HAMA and GelMA separately within hybrid hydrogels, we can induce changes in hydrogel properties. Varying polymer concentrations in hydrogels demonstrated a consistently high viability of encapsulated VICs. However, proliferation rate was significantly decreased in 5% (w/v) GelMA hydrogels. VICs encapsulated in these hydrogels demonstrated a spread-like morphology, which was absent in other conditions that demonstrated a more rounded cell morphology. Our data indicated that VIC activation and subsequent myofibroblast-like differentiation only occurred in the relatively soft 5% (w/v) GelMA hydrogel environment. When HAMA is added to the 5% (w/v) GelMA hydrogels, VICs remain quiescent. However, the addition of TGFβ1 to the VICs within 1% (w/v) HAMA-5% (w/v) GelMA hydrogels led to myofibroblast-like differentiation. These results indicate that hybrid hydrogels can be used to maintain VICs in a quiescent phenotype, which can controllably be activated to undergo myofibroblast-like activation. Hence, hybrid hydrogels provide for a platform to study VIC phenotypic changes as they may occur in the heart valve.

The results of this study extend the evidence that VIC myofibroblast-like differentiation is not solely driven by increased stiffness as is observed in tissue culture,[6b,7,22] but that also more compliant microenvironments can facilitate VIC activation. Interestingly, the aortic heart valve leaflet was initially considered to have a relatively stiff modulus of 1.74 ± 0.29 MPa,[23] which seemed to increase while the valve becomes more fibrotic over time, driving observed myofibroblast-like differentiation of VICs in vivo. However, recent evidence has demonstrated that the modulus of the valve ECM may be layer specific, as the aortic valve leaflet consists of three distinct ECM layers characterized by specific ECM proteins; the zona fibrosa, which predominantly consists of collagen, zona spongiosa, mostly containing GAGs, and the zona ventricularis, characterized by elastin.[1b] Micropipette aspiration indicated that the modulus of the zona ventricularis was ≈3 kPa and the zona fibrosa was ≈5 kPa.[24] In our study, 5% (w/v) GelMA hydrogels demonstrated a modulus of 5.7 ± 2.3 kPa corresponding to the modulus of the zona fibrosa. Considering that pathological changes, including calcification, preceded by myofibroblast-like

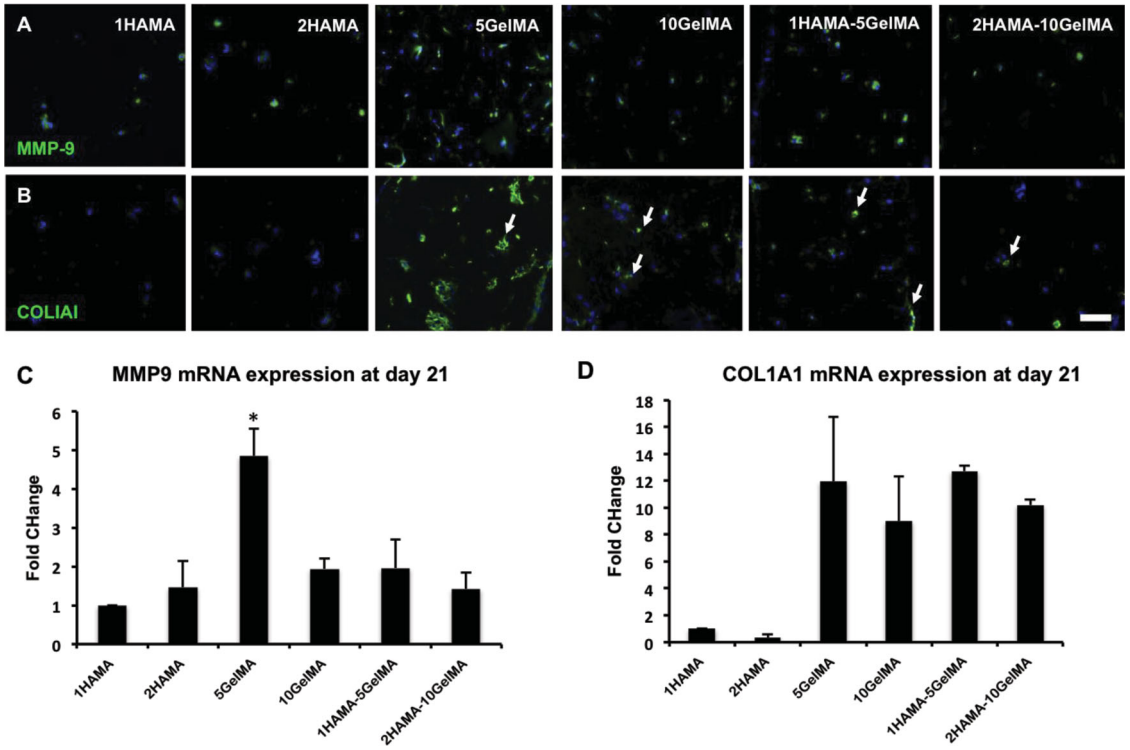

Figure 5. Hydrogel composition affects VIC behavior at day 21. A) Immunofluorescence staining of metallomatrixproteinase-9 (MMP-9), MMP9: green, nuclei: blue. B) Immunofluorecence staining of collagen type 1 (COL1A1), COL1A1: green, nuclei: blue. C) mRNA expression assessed by RT-PCR of MMP-9. D) Collagen type I (COL1A1). Expression is depicted as mean ± SD fold change to 1% (w/v) HAMA.* $p < 0.05$.

differentiation of VICs, most often occur in the zona fibrosa,[1b] makes our 3D hydrogel platform clinically relevant.

Similar results were demonstrated by another recent study that explored the use of HAMA and GelMA as a composite hydrogel platform.[16] By altering the molecular weight of HA, Duan et al. varied the physical properties of their composite hydrogels. However, although an increased spread-like morphology was observed in their HAMA hydrogels containing GelMA, myofibroblast differentiation was only observed in hydrogels consisting of HAMA alone. We do not observe any myofibroblast differentiation in HAMA hydrogels. An explanation for this difference with our study might be that the difference in physical properties between our hydrogel conditions is more pronounced with moduli ranging from 5kPa to 120 kPA, leading to more apparent differences in VIC response. Further, our study indicates that quiescent VICs in hydrogels can be activated by the addition of TGFβ1. This observation is important because it indicates that these gels may be utilized as a model system to study known cytokine initiators of valve disease independently of VIC phenotypic changes caused by the culture environment.

Studies have shown that local mechanical properties of the ECM regulate cellular motility, proliferation, and differentiation.[8] More specifically, cells intrinsically generate cytoskeletal tension as they exert tractional forces on the surrounding matrix; stiff matrices provide greater resistance to deformation, resulting in greater tractional forces.[8] Incorporation of α-SMA into the stress fibers aids in force generation[25] that becomes apparent when VICs are cultured on stiff tissue culture polystyrene plates. This suggests that VICs in our hydrogels would demonstrate increased α-SMA when faced with greater resistance due to stiffness.

The correlation between hydrogel stiffness and polymer crosslinking density[26] could explain the lack of myofibroblast-like differentiation in stiffer hydrogels. Decreasing polymer density, and thus the number of peptides that must be cleaved to permit cell spreading and motility, could facilitate spreading and thus differentiation[14b,21] as there may be more space for VICs to extend outwards and exert tractional force. This may explain why VICs exhibit an activated phenotype in the 5% (w/v) GelMA hydrogels but are unable to spread and therefore, do not undergo the same phenotypic changes in the denser 10% (w/v) GelMA hydrogels. However, this phenomenon may also be aided by the increased degradation rate of softer, less dense 5% (w/v) GelMA hydrogels,[21] whereas 10% (w/v) GelMA hydrogels degrade slower and may thus hinder VIC myofibroblast-like differentiation and associated cell spreading. Hence, it remains to be elucidated to what extent material stiffness and degradation contribute to VIC phenotypical fate. An additional component to consider is the interaction of HA and VICs itself. Studies have shown that disruption of VIC–HA interaction may enhance myofibroblast-like differentiation of VICs, indicating HA could be crucial in maintaining a healthy quiescent VIC phenotype.[27]

After confirming a quiescent VIC phenotype in the hybrid 1% (w/v) HAMA-5% (w/v) GelMA hydrogel, we further assessed the possibility of controllable VIC activation with biochemical cues. TGFβ1 is expressed in pathological aortic valves

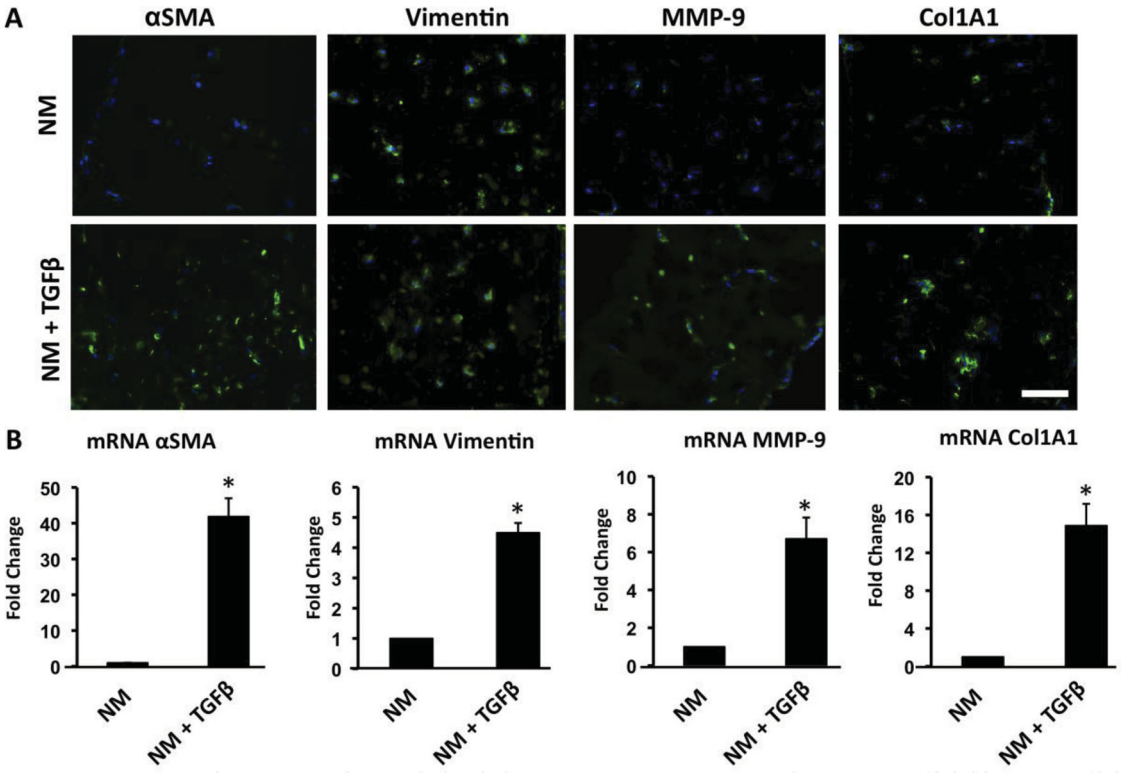

Figure 6. Activation of quiescent VICs by TGFβ. TGFβ1 was exogenously added to VICs cultured in 1% (w/v) HAMA-5% (w/v) GelMA. A) Immunofluorescence (αSMA, vimentin MMP-9 COL1A1 = green, nuclei = blue) bar: 50 µm. B) RT-PCR of mRNA expression of α-SMA, vimentin, MMP-9, COL1A1. Data are depicted as mean fold change ± SD compared to control (normal media), * $p < 0.05$.

and is a known potent inducer of myofibroblast differentiation of VICs both in 2D[13] and 3D cultures.[15a] TGFβ1 is latent when secreted and stored in the valvular ECM. Matrix cues such as increased strain may result in the activation of TGFβ1 and subsequent myofibroblast activation of VICs. Moreover, TGFβ1-dependent induction of pathologic differentiation of VICs seems to be dependent on stretching the ECM.[28] TGFβ1 is a relevant biochemical factor that may work alongside biomechanical forces in leading to VIC differentiation; however, utilizing a hybrid approach, encapsulating VICS in these hydrogels can allow for these biochemical affects to be studied specifically.

The approach to model VIC phenotypic transition in the present study is limited by the static nature of the hydrogel platform. Valves are dynamic organs exposed to repetitive strain and stress during the cardiac cycle.[1b] Thus, adding a dynamic component to a hydrogel platform would be warranted. In addition, a true in vitro valve model would also entail an endothelial monolayer as observed in the native valve. The advantage of including HAMA in a hybrid hydrogel platform is that although HA is void of cell adhesion motifs like collagen-like substrate, it is a GAG, which is abundantly present in the *zona spongiosa* of the valve ECM,[24] which makes a hybrid hydrogel better suitable to mimic valve ECM to study VIC behavior in a 3D culture platform.

In conclusion, we have utilized the combination of naturally derived polymers HAMA and GelMA into a hybrid hydrogel platform, which can be used to study VIC phenotypic fate. By encapsulating VICs in a hybrid HAMA–GelMA hydrogel, we could facilitate and maintain a quiescent VIC phenotype, which upon stimulation with TGFβ1, were able to differentiate into myofibroblast-like cells. Thus, we present here a 3D hybrid-hydrogel system that could serve as controllable model to study the mechanisms of transition from quiescent to activated myofibroblast-like VICs, in a more analogous in vivo environment of native heart valve tissue. The results of this study may aid in the development of adequate valvular disease platforms or drug discovery tools.

4. Experimental Section

Synthesis of Materials: HAMA was synthesized as described previously.[20] Briefly, methacrylic anhydride (Sigma–Aldrich, St. Louis, MO) was added to a solution of 1 wt% hyaluronic acid (53 kDA, Lifecore Biomedical, Chaska, MN) in distilled water. The pH was adjusted to 8 using 5 M NaOH (Sigma–Aldrich) and kept on ice during the reaction for 24 h. The HAMA solution was dialyzed against deionized water for 72 h after which lyophilization was performed, resulting in a solid white foam-like material that was stored at –80 °C prior to experimental use. The methacrylation degree of ≈20% was determined by ^{1}H NMR. The synthesis of GelMA has also been reported before.[14b,21] Powdered type A cell culture tested gelatin from porcine skin (Sigma–Aldrich) was dissolved in phosphate buffered saline and heated at 60 °C under continuous stirring for 20 min to obtain a 10 wt% gelatin solution. After dropwise addition of 8% (v/v) methacrylic anhydride under constant stirring for 3 h at 50 °C, GelMA solution was diluted and dialyzed against deionized water at 40 °C for 1 week. This yielded a methacrylation degree

DOI: 10.1002/adhm.201400029

of ≈80% as determined by ^{1}H NMR. Finally, the solution was lyophilized for 1 week, yielding a white porous foam-like substance, which was stored at –80 °C before experimental use.

Hydrogel Fabrication: Hydrogels were fabricated from HAMA and GelMA using photocrosslinking (Figure 1A–C). First, a 0.5% photoinitiator (PI) solution was prepared by dissolving 5 mg PI (Igracure 2595) in 1 mL of phosphate buffered saline (PBS; Gibco) at 80 °C. Solutions of 1 wt% HAMA, 2 wt% HAMA, and 5 wt% GelMA, 10 wt% GelMA, 1 wt% HAMA-5 wt% GelMA, and 2 wt% HAMA-10 wt% GelMA with 1 mL PI solution were placed in an 80 °C oven for 20 min to yield respective prepolymer solutions. Hydrogels were formed by pipetting 50 µL of prepolymer solution between two 450 µm spacers and exposed to 2.5 mW cm^{-2} UV light (Omnicure S2000, EXFO Photonic Solutions Inc., Ontario, Canada; wavelength 320–480 nm) for 30 s. The exposure to light facilitates crosslinking of the polymers in the solution yielding a disc-shaped hydrogel with a height of 450 µm (Figure 1B,C). Unreacted polymer was then rinsed away with PBS.

Hydrogel Characterization: The porosity of the hydrogel conditions was visualized using scanning electron microscopy (SEM) (Cold field-emission gun scanning electron microscope (FEG-SEM), JEOL 6700F)). Samples were prepared by freezing fully hydrated hydrogels in liquid nitrogen followed by lyophilization. The samples were broken in half to allow for imaging of cross-sections. The lyophilized samples were then coated with Pt/Pd before imaging. Pore size was quantified by determining equivalent circle diameter (ECD) with Image J of at least 50 pores from five SEM images made from three hydrogels per condition. Porosity was also examined using swelling analysis. Photocrosslinked hydrogels were placed in Eppendorf tubes containing 1 mL of PBS for 24 h to reach equilibrium swelling. The wet weight of the swollen hydrogels was determined after gently blotting excess liquid with kimwipes. The hydrogels were frozen and lyophilized to enable the measurement of the dry weight. Swelling ratio was determined by calculating (wet weight–dry weight)/dry weight. Five replicates were made for each hydrogel composition. For mechanical testing, 100 µL prepolymer solution (0.5% PI) was added between 1 mm spacers and exposed to 90 s of 2.5 mW cm^{-2} UV light. After rinsing with PBS, hydrogels were stored in PBS at 4 °C for 24 h. Prior to mechanical testing, hydrogels were punched with a 8-mm biopsy punch and excess liquid was removed. A strain rate of 0.2 mm min^{-1} was applied using an Instron 5542. The compressive modulus (kPa) was determined by taking the slope in the linear section of stress–strain curve at 10%–15% strain area. Five hydrogels were tested for each condition.

VIC Isolation and Culture: Aortic valve leaflets were obtained from hearts of 10-month-old pigs sacrificed at a USDA-approved abattoir (THOMA Meat Market, Saxonburg, PA). Within 3 h after dissection, valve surfaces were scraped to remove endothelial cells. VICs were isolated from valve leaflets using collagenase A (Sigma, St. Louis, MO) digestion. Cells were cultured in normal growth medium containing Dulbecco's modified Eagle's medium (DMEM) with 10% fetal bovine serum and 1% penicillin/streptomycin (Invitrogen, Grand Island, NY). Cells between passages 3 and 6 were used for all experiments. After culture, VICs were encapsulated in hydrogel constructs and cultured for up to 21 d at 37 °C, 5% CO_2.

VIC Encapsulation: Prepolymer solutions were prepared for each condition as described above. The solutions were vortexed regularly. The polymer solution was then allowed to cool to 37 °C. VICs at 80% confluency were trypsinized and centrifugated at 1500 rpm for 5 min. The supernatant was aspirated and the remaining cell pellet was resuspended in the prepolymer solution at a density of 10 million cells mL^{-1}. Fifty microliters of the cell-laden prepolymer solution was dropwise added to a petri-dish between two spacers with a height of 450 µm and covered with an autoclaved sterile glass slide. The cell-laden solution was then subjected to 2.5 mW cm^{-2} UV light (Omnicure S2000, EXFO Photonic Solutions Inc., Ontario, Canada; wavelength 320–500 nm) for 30 s, resulting in photocrosslinked VIC-laden hydrogel (Figure 1A–C). The hydrogel was removed from the glass slide and put into a well plate containing normal growth medium. For selected experiments, transforming growth factor β1 (TGFβ1) (R&D systems, Minneapolis, MN) was added at a concentration of 5 ng mL^{-1}. Medium was changed every 48 h.

Cell Viability, Proliferation, and Apoptosis: Cell viability was determined by fluorescent labeling with 4×10^{-6} M calcein AM and 2×10^{-6} M ethidium homodimer-1 (LIVE/DEAD Viability kit for mammalian cells, Invitrogen). Cell-laden hydrogels were first washed with PBS for 5 min and then incubated with fluorescent dye for 20 min at room temperature. The cell-laden hydrogels were then washed with PBS and imaged using a confocal microscope (Nikon Instruments, Inc. A1/C1 Confocal Microscope). Three hydrogels were analyzed each time point for each condition. Of each hydrogel, three z-stacks (10 µm per slice) were made of which a compressed image was formed. Viable cells were stained green and dead cells red, and the numbers of each type were manually counted using Image J Software. Data are depicted as percentage of live cells. To quantifiably analyze spreading of encapsulated VICs, mean cell surface area was determined from 3D reconstruction of the confocal z-stacks using MATLAB. Proliferation of VICs encapsulated in the hydrogels was assessed by EdU labeling. EdU binds to cell nuclei when they are in the S-phase of the cell cycle, making it highly specific assay for proliferation. First, VIC-laden hydrogels were incubated with 10×10^{-6} M EdU for 12 h on days 1, 7, 14 and 21. Samples were then fixed and permeabilized using a Fixation and Permeabilization kit (Invitrogen/Life technologies) and subsequently washed with a 1% BSA solution in PBS, after which constructs were incubated with Click-iT solution (350 µL) from the Click-iT EdU Alexa Fluor 488 kit (Invitrogen/Life technologies) for 30 min at room temperature. Cell nuclei were counterstained with DAPI. Cell-laden hydrogels were then analyzed by confocal microscopy. Three z-stacks were made per cell-laden hydrogel. Proliferation was assessed by ImageJ quantification of positively labeled cells of compressed images of the z-stacks. VICs in culture for 24 h were stained at the same time using similar protocol for positive control. Three hydrogels were analyzed for each time point per using an EdU labeling kit (Invitrogen). Data are depicted as mean percentage of proliferating cells and mean cell number per high power field (HPF) magnification (×20). Apoptosis was determined by TUNEL (terminal deoxynucleotidyl transferase mediated dUTP nick end labeling) staining (Millipore, Remecula, CA, USA), according to the manufacturer's protocol and quantified using fluorescence microscopy. Data are depicted as percentage of positively stained cells.

Histological Evaluation of 3D Cell-Laden Hydrogel Constructs: Cell-laden hydrogels were washed with PBS for 5 min and then fixed in 4% paraformaldehyde for 20 min, followed by PBS wash. The hydrogels were kept in a 30 wt% sucrose solution overnight at 4 °C, after which they were frozen in OCT compound (Sakura Finetech, Torrance, CA) and 10 µm sections were cut. For comparison, VICs cultured in 2D on TCPS were fixed after 24 h in 4% paraformaldehyde for 15 min followed by PBS wash. Immunofluorescence staining for α-SMA, vimentin, matrix-metalloproteinase-9 (MMP-9), and Collagen type I (Col-I) was performed. VIC-laden hydrogel sections and VICs (2D) were permeabilized using 0.1% Triton-X. After blocking in 4% horse serum, sections were incubated with monoclonal mouse anti α-SMA primary antibody (Clone 1A4, Dako, Dako Denmark A/S, Glostrup, Denmark), a monoclonal mouse anti-vimentin primary antibody (Abcam, Cambridge, USA), a monoclonal mouse anti-MMP9 (Santa Cruz), or a monoclonal mouse-anti COL-1 (Abcam, Cambridge, USA) for 90 min at room temperature (RT), followed by biotin-labeled secondary antibody (Vector Labs, Burlingame, CA, USA) for 45 min at RT and streptavidin-labeled AlexaFluor 488 (Invitrogen, Grand Island, NY, USA) for 20 min at RT. Sections were washed three times in PBS for 5 min and nuclei were counterstained with DAPI containing mounting medium (Vector Labs, Burlingame, CA, USA). Images were taken with an Eclipse 80i microscope (Nikon, Melville, NY, USA) and processed with Elements 3.20 software (Nikon, Melville, NY, USA). Positive staining was quantified by manually counting positively stained cells of the total cell number in five HPFs per hydrogel. Three hydrogels were quantified per condition per time point.

Real-Time Polymerase Chain Reaction for Expression of Cell Markers: RNA from encapsulated VICs was isolated from cell-laden hydrogels

by mechanical disruption of the hydrogels (TissueLyzer, Qiagen, Germany). Total RNA was isolated from using GE Healthcare RNAspin mini RNA Isolation kit. The amount of RNA in each sample was measured using NanoDrop 2000c (ThermoScientific). Total RNA was reverse transcribed with oligo-(dT)12–18 primers(Invitrogen/Life Technologies, Grand Island, NY, USA) and Superscript II reverse transcriptase (Invitrogen/Life Technologies, Grand Island, NY, USA) to obtain a target cDNA concentration of 0.335 μg mL^{-1} followed by Real Time-Polymerase Chain Reaction (RT-PCR) using SYBR Green (BioRad, Hercules, CA, USA), and annealing temperatures of 95 °C and 60 °C 35 cycles. Primer sequences were designed with Primer3 software and were as follows: α-SMA: F:5′-AGTGCGACATTGACATCAGG-3′ and R:5′-CTGGAAGGTGGACAGAGAGG-3′, vimentin F:5′-AGCAGTATGAGAGTGTGGCC-3′and R:5′-CTTCCATTTCCCGCATCTG**G**-3′, MMP-9 F:5′GGTGGACTATGTGGGCTACG-3′ and R:5′-AGTGCTGAAGCAGGACGAG-3′, and Collagen type 1 F:5′-CCAAGAGGAGGGCCAAGAAGAAGG-3′ and R:5′-GGGGCAGACGGGGCAGCACTC-3′. The housekeeping gene used was glyceraldehyde-3-phosphate dehydrogensase (GAPDH): F:5′-CCCAGAAGACTGTGGATGG-3′, R:5′-ACCTGGTCCTCAGTGTAGCC-3′. Expression was quantified using comparative Ct (Cycle threshold method $2^{-\Delta\Delta CT}$ method) with the following equations: 1) ΔCT = CT of target gene –CT of housekeeping gene, 2) ΔΔCT = ΔCT day *x* – ΔCT day 1; 3) Fold increase between groups = $2^{-\Delta\Delta Ct}$

Statistical Analysis: Results are presented as mean ± standard deviation unless indicated otherwise. One-way ANOVA was used to evaluate statistical significant differences in multiple groups. A value of $p < 0.05$ was considered significant.

Supporting Information

Supporting Information is available from the Wiley Online Library or from the author.

Acknowledgements

The authors acknowledge the Netherlands Heart Foundation (NHF-2011T024) and Netherlands Scientific Council (NWO-92003572) to J.H., and NIH R01HL114805 and NIH R01HL109506 to E.A. A.K. acknowledges the Office of Naval Research Young National Investigator Award, the Presidential Early Career Award for Scientists and Engineers (PECASE), the National Science Foundation CAREER Award (DMR 0847287), and the National Institutes of Health (EB012597, HL092836, HL099073, EB008392).

Received: January 13, 2014
Revised: March 20, 2014
Published online:

[1] a) E. Rabkin, M. Aikawa, J. R. Stone, Y. Fukumoto, P. Libby, F. J. Schoen, *Circulation* **2001**, *104*, 2525; b) F. J. Schoen, *Circulation* **2008**, *118*, 1864.
[2] a) E. Aikawa, M. Nahrendorf, D. Sosnovik, V. M. Lok, F. A. Jaffer, M. Aikawa, R. Weissleder, *Circulation* **2007**, *115*, 377; b) E. Aikawa, M. Aikawa, P. Libby, J. L. Figueiredo, G. Rusanescu, Y. Iwamoto, D. Fukuda, R. H. Kohler, G. P. Shi, F. A. Jaffer, R. Weissleder, *Circulation* **2009**, *119*, 1785.
[3] a) E. R. Mohler 3rd, F. Gannon, C. Reynolds, R. Zimmerman, M. G. Keane, F. S. Kaplan, *Circulation* **2001**, *103*, 1522; b) C. M. Otto, *N. Engl. J. Med.* **2008**, *359*, 1395; c) N. M. Rajamannan, F. J. Evans, E. Aikawa, K. J. Grande-Allen, L. L. Demer, D. D. Heistad, C. A. Simmons, K. S. Masters, P. Mathieu, K. D. O'Brien, F. J. Schoen, D. A. Towler, A. P. Yoganathan, C. M. Otto, *Circulation* **2011**, *124*, 1783.
[4] N. M. Rajamannan, M. Subramaniam, S. R. Stock, N. J. Stone, M. Springett, K. I. Ignatiev, J. P. McConnell, R. J. Singh, R. O. Bonow, T. C. Spelsberg, *Heart* **2005**, *91*, 806.
[5] C. A. Simmons, G. R. Grant, E. Manduchi, P. F. Davies, *Circulation Res.* **2005**, *96*, 792.
[6] a) A. M. Kloxin, J. A. Benton, K. S. Anseth, *Biomaterials* **2010**, *31*, 1; b) A. M. Quinlan, K. L. Billiar, *J. Biomed. Mater. Res. Part A* **2012**, *100*, 2474; c) K. Wyss, C. Y. Yip, Z. Mirzaei, X. Jin, J. H. Chen, C. A. Simmons, *J. Biomech.* **2012**, *45*, 882.
[7] J. H. Chen, C. A. Simmons, *Circulation Res.* **2011**, *108*, 1510.
[8] D. E. Discher, P. Janmey, Y. L. Wang, *Science* **2005**, *310*, 1139.
[9] a) D. Choquet, D. P. Felsenfeld, M. P. Sheetz, *Cell* **1997**, *88*, 39; b) H. B. Wang, M. Dembo, S. K. Hanks, Y. Wang, *Proc. Natl. Acad. Sci. U.S.A.* **2001**, *98*, 11295.
[10] D. E. Ingber, *FASEB J.* **2006**, *20*, 811.
[11] J. J. Tomasek, G. Gabbiani, B. Hinz, C. Chaponnier, R. A. Brown, *Nat. Rev. Mol. Cell Biol.* **2002**, *3*, 349.
[12] a) P. M. Taylor, S. P. Allen, S. A. Dreger, M. H. Yacoub, *J. Heart Valve Disease* **2002**, *11*, 298; b) I. Ben-Dor, A. D. Pichard, M. A. Gonzalez, G. Weissman, Y. Li, S. A. Goldstein, P. Okubagzi, A. I. Syed, G. Maluenda, S. D. Collins, C. Delhaye, K. Wakabayashi, M. A. Gaglia Jr., R. Torguson, Z. Xue, L. F. Satler, W. O. Suddath, K. M. Kent, J. Lindsay, R. Waksman, *Circulation* **2010**, *122*, S37.
[13] G. A. Walker, K. S. Masters, D. N. Shah, K. S. Anseth, L. A. Leinwand, *Circulation Res.* **2004**, *95*, 253.
[14] a) B. V. Slaughter, S. S. Khurshid, O. Z. Fisher, A. Khademhosseini, N. A. Peppas, *Adv. Mater.* **2009**, *21*, 3307; b) J. W. Nichol, S. T. Koshy, H. Bae, C. M. Hwang, S. Yamanlar, A. Khademhosseini, *Biomaterials* **2010**, *31*, 5536.
[15] a) J. A. Benton, B. D. Fairbanks, K. S. Anseth, *Biomaterials* **2009**, *30*, 6593; b) J. A. Benton, C. A. DeForest, V. Vivekanandan, K. S. Anseth, *Tissue Eng. Part A* **2009**, *15*, 3221; c) D. N. Shah, S. M. Recktenwall-Work, K. S. Anseth, *Biomaterials* **2008**, *29*, 2060.
[16] B. Duan, L. A. Hockaday, E. Kapetanovic, K. H. Kang, J. T. Butcher, *Acta Biomater.* **2013**, *9*, 7640.
[17] K. S. Masters, D. N. Shah, L. A. Leinwand, K. S. Anseth, *Biomaterials* **2005**, *26*, 2517.
[18] S. T. Kreger, S. L. Voytik-Harbin, *Matrix Biol.: J. Int. Soc. Matrix Biol.* **2009**, *28*, 336.
[19] J. L. Ifkovits, E. Tous, M. Minakawa, M. Morita, J. D. Robb, K. J. Koomalsingh, J. H. Gorman, 3rd, R. C. Gorman, J. A. Burdick, *Proc. Natl. Acad. Sci. U.S.A.* **2010**, *107*, 11507.
[20] G. Camci-Unal, H. Aubin, A. F. Ahari, H. Bae, J. W. Nichol, A. Khademhosseini, *Soft Matter* **2010**, *6*, 5120.
[21] G. Camci-Unal, D. Cuttica, N. Annabi, D. Demarchi, A. Khademhosseini, *Biomacromolecules* **2013**, *14*, 1085.
[22] C. Y. Yip, M. C. Blaser, Z. Mirzaei, X. Zhong, C. A. Simmons, *Arteriosclerosis Thrombosis Vascular Biol.* **2011**, *31*, 1881.
[23] P. Stradins, R. Lacis, I. Ozolanta, B. Purina, V. Ose, L. Feldmane, V. Kasyanov, *Eur. J. Cardio-Thoracic Surgery* **2004**, *26*, 634.
[24] R. Zhao, K. L. Sider, C. A. Simmons, *Acta Biomater.* **2011**, *7*, 1220.
[25] B. Hinz, G. Celetta, J. J. Tomasek, G. Gabbiani, C. Chaponnier, *Mol. Biol. Cell* **2001**, *12*, 2730.
[26] C. Cha, W. B. Liechty, A. Khademhosseini, N. A. Peppas, *ACS Nano* **2012**, *6*, 9353.
[27] K. J. Rodriguez, L. M. Piechura, K. S. Masters, *Matrix Biol.: J. Int. Soc. Matrix Biol.* **2011**, *30*, 70.
[28] a) J. D. Hutcheson, V. Setola, B. L. Roth, W. D. Merryman, *Pharmacol. Ther.* **2011**, *132*, 146; b) W. D. Merryman, H. D. Lukoff, R. A. Long, G. C. Engelmayr Jr., R. A. Hopkins, M. S. Sacks, *Cardiovascular Pathol.* **2007**, *16*, 268.